Department of Geophysics
Graduate School of Science, Tohoku University

Vertical-Wind-Induced Cloud Opacity Variation in Low Latitudes Simulated by a Venus GCM

Hiroki Karyu[1], Takeshi Kuroda[1], Kazunari Itoh[1], Akira Nitta[1], Kohei Ikeda[2], Masaru Yamamoto[3], Norihiko Sugimoto[4,5], Naoki Terada[1], Yasumasa Kasaba[1,6], Masaaki Takahashi[7], and Paul Hartogh[8]

[1]Department of Geophysics, Tohoku University, Sendai, Japan, [2] National Institute for Environmental Studies, Tsukuba, Japan, [3]Research Institute for Applied Mechanics, Kyushu University, Kasuga, Japan, [4]Department of Physics, Keio University, Yokohama, Japan, [5]Research and Education Center for Natural Sciences, Keio University, Yokohama, Japan, [6]Planetary Plasma and Atmospheric Research Center, Tohoku University, Sendai, Japan, [7]Atmosphere and Ocean Research Institute, The University of Tokyo, Kashiwa, Japan, [8]Max Planck Institute for Solar System Research, Goettingen, Germany.

Importance of Atmospheric Wave

Atmospheric wave is a key to understand dynamics and meteorology

Earth (McCormack et al., 2021)

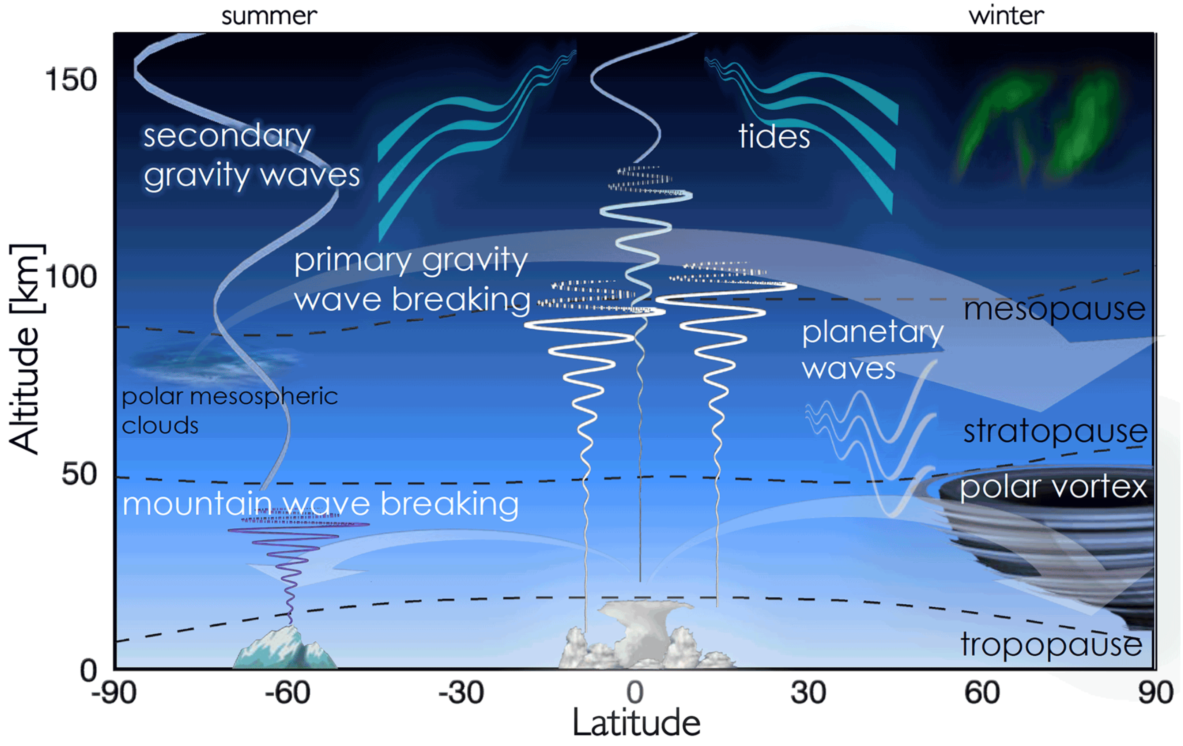

Venus

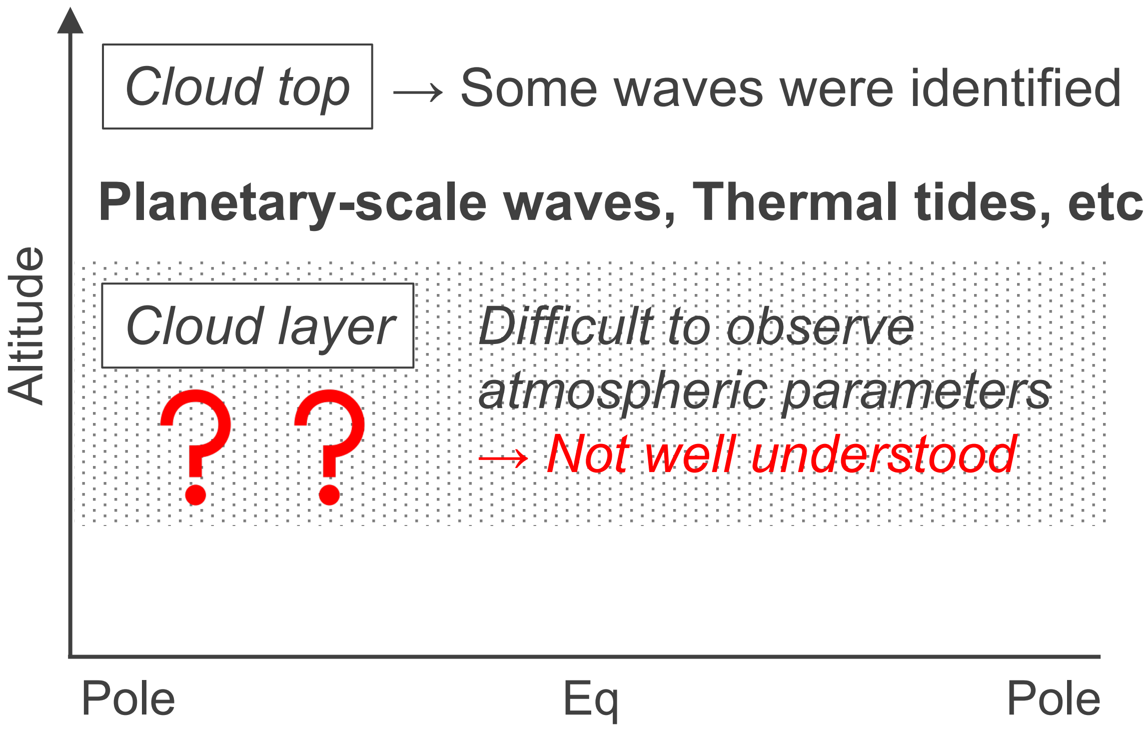

However, atmospheric wave activities in the Venusian cloud layer are not well understood due to the difficulty of continuous observation

Venusian Cloud Morphology

Cloud morphology can be used as a diagnostic tool of atmospheric dynamics

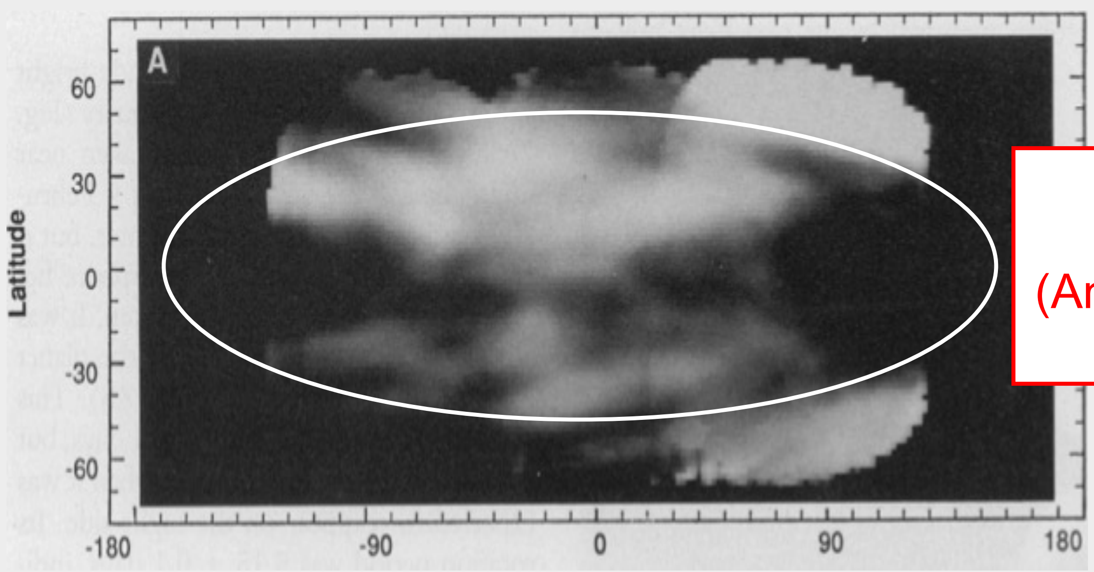

Coupled?
(Ando et al., 2021)

Kelvin wave (Matsuno, 1966)
Planetary-scale wave found in the equatorial region

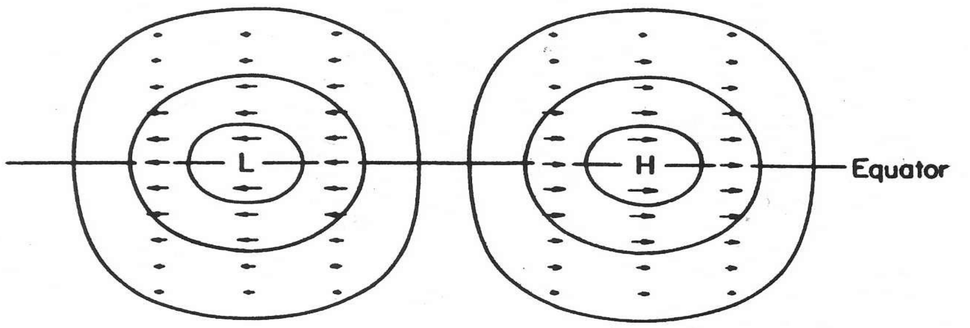

- Crisp et al. (1991) found a zonal-wavenumber-1 cloud opacity variation in low latitudes
- The variation quasi-periodically moved westward and persisted for a few weeks

- *Can a Kelvin wave explain the observed cloud variation?*

Setup of the GCM

Venus General Circulation Model (GCM) used in this study

- Dynamical core is based on CCSR/NIES GCM (Numaguti et al., 1995), which is also applied to a Mars GCM (Kuroda et al., 2005)
- Resolution: T42 (128 x 64 grids), 52 vertical layers (0~95 km)
- Dynamical settings are taken from Yamamoto et al. (2019, 2021)

→ Wind and thermal structures are identical to Yamamoto et al.

- Topography is not included
- A radiative transfer scheme is taken from Ikeda (2011)
- Cloud physics parameterization including Mode 1~3

→ condensation/evaporation, sedimentation

- Simple chemistry that represents H_2SO_4 cycle

Dynamical settings

Parameter	Value
Planet radius	6051.848 km
Gravity acceleration	8.87 m s^{-2}
Planetary rotation period	243 Earth days
Length of solar day	117 Earth days
Gas constant	191.4 J kg^{-1} K^{-1}
Solar constant	2607 W m^{-2}
Specific heat at the constant pressure	8.6 – 10.9 × 10^2 J kg^{-1} K^{-1}
Surface drag coefficient	4 × 10^{-3}
Vertical eddy diffusion for momentum and heat	0.8 m^2 s^{-1}
Vertical eddy diffusion for tracers	0.2 – 4 m^2 s^{-1}

The rotation setting is the opposite of the actual Venus in the present study (SR is prograde)

Cloud formations

Cloud production

1. H_2SO_4 formation by simple chemical reactions
2. Condensation is determined by the saturation vapor pressure of H_2SO_4
3. The liquid H_2SO_4 and H_2O (75% H_2SO_4) form cloud droplets, and the particle sizes are determined by a priori size ratio (right fig.) (Haus and Arnold, 2010)

(Particle size evolution is not calculated)

Cloud sedimentation

- Stokes velocity

$$w_{sed} = \frac{2\rho_p g r^2}{9\mu}\left[1 + \frac{\lambda}{r}\left(A + B\exp\left\{-\frac{Cr}{\lambda}\right\}\right)\right],$$

$$F_{sed} = -q_i w_{sed},$$

ρ_p: particle density, r: radius, λ: mean free path, μ: viscosity, A, B, C: experimental parameters from Kasten (1968)

Mode	1	2	2’	3
Radius (μm)	0.49	1.18	1.40	3.65
Velocity (m/day)	~5	~25	~50	~400

← ~ 1 bar

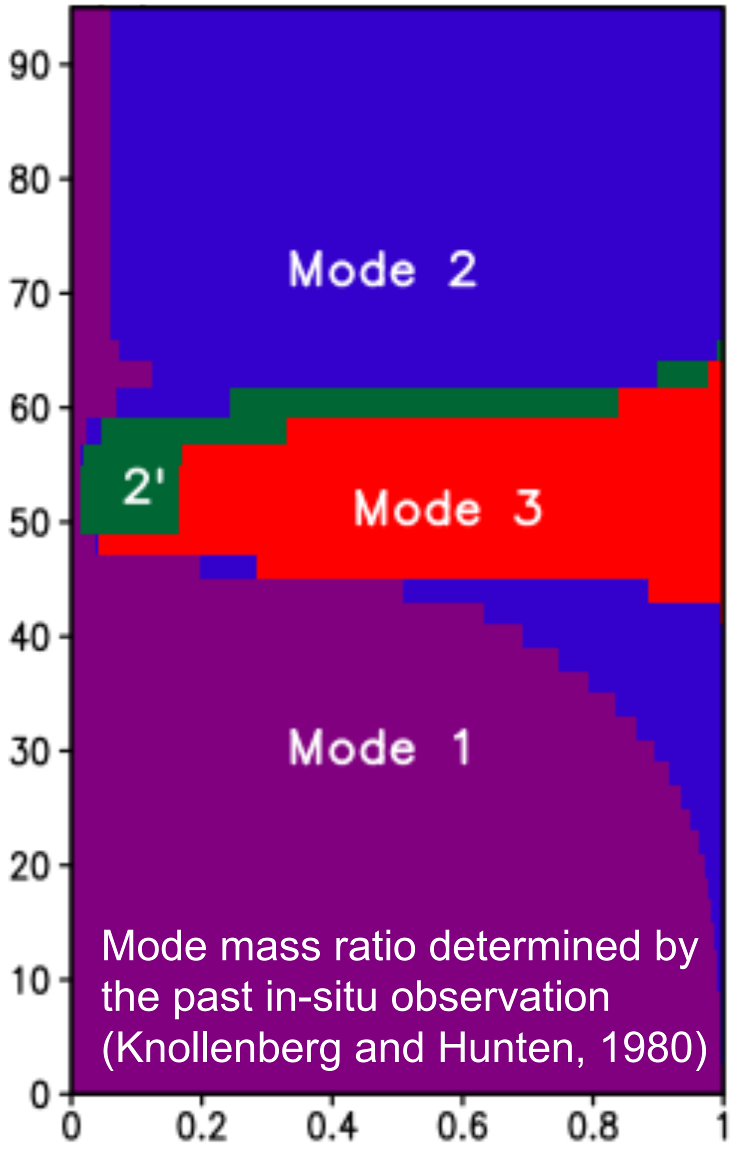

Mode mass ratio determined by the past in-situ observation (Knollenberg and Hunten, 1980)

Implemented chemical reactions

Chemical reactions (shown in the table below)

- SO_2: linear relaxation to the reference profile (right fig.) following Marcq and Lebonnois (2013)
- O: fixed to a reference profile which is proportional to solar zenith angle (representing photochemistry)
- CO: fixed
- SO_3, H_2SO_4, H_2O: calculated

Reaction	Reaction coefficient
$SO_2 + O + M \rightarrow SO_3 + M$	$k_1 = 5\times10^{-22} T^{-3} \exp\left(-\frac{2400}{T}\right)$
$SO_3 + H_2O + H_2O \rightarrow H_2SO_4 + H_2O$	$k_2 = 2.3\times10^{-43} T \exp\left(\frac{6540}{T}\right)$
$H_2SO_4 + H_2O \rightarrow SO_3 + H_2O + H_2O$	$k_3 = 7\times10^{-14} \exp\left(-\frac{5170}{T}\right)$
$SO_3 + CO \rightarrow SO_2 + CO_2$	$k_4 = 10^{-11} \exp\left(-\frac{13000}{T}\right)$

Initial vertical profiles

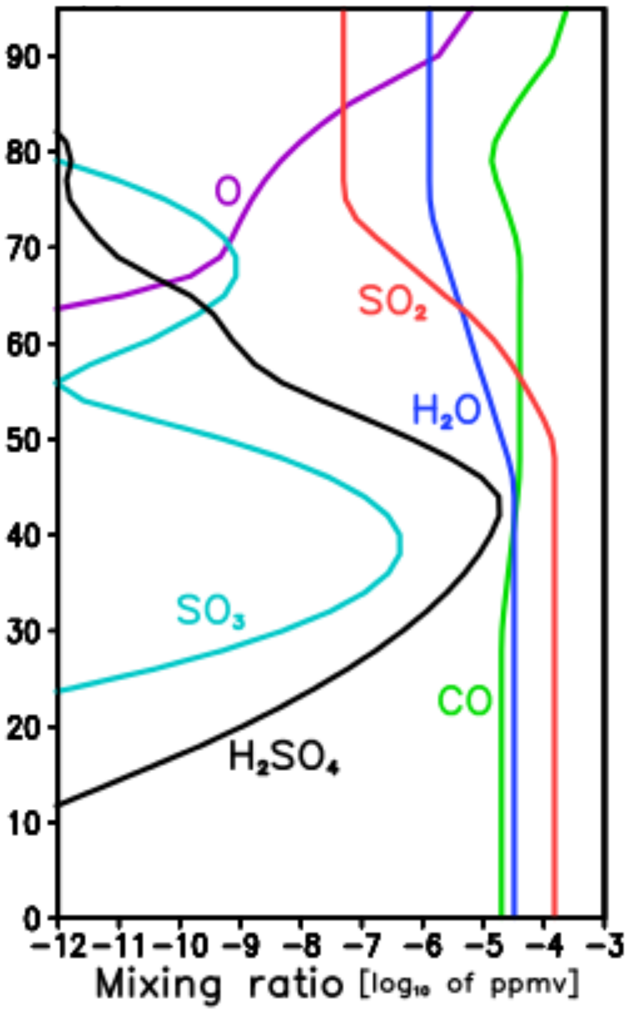

Zonal mean wind and thermals structure

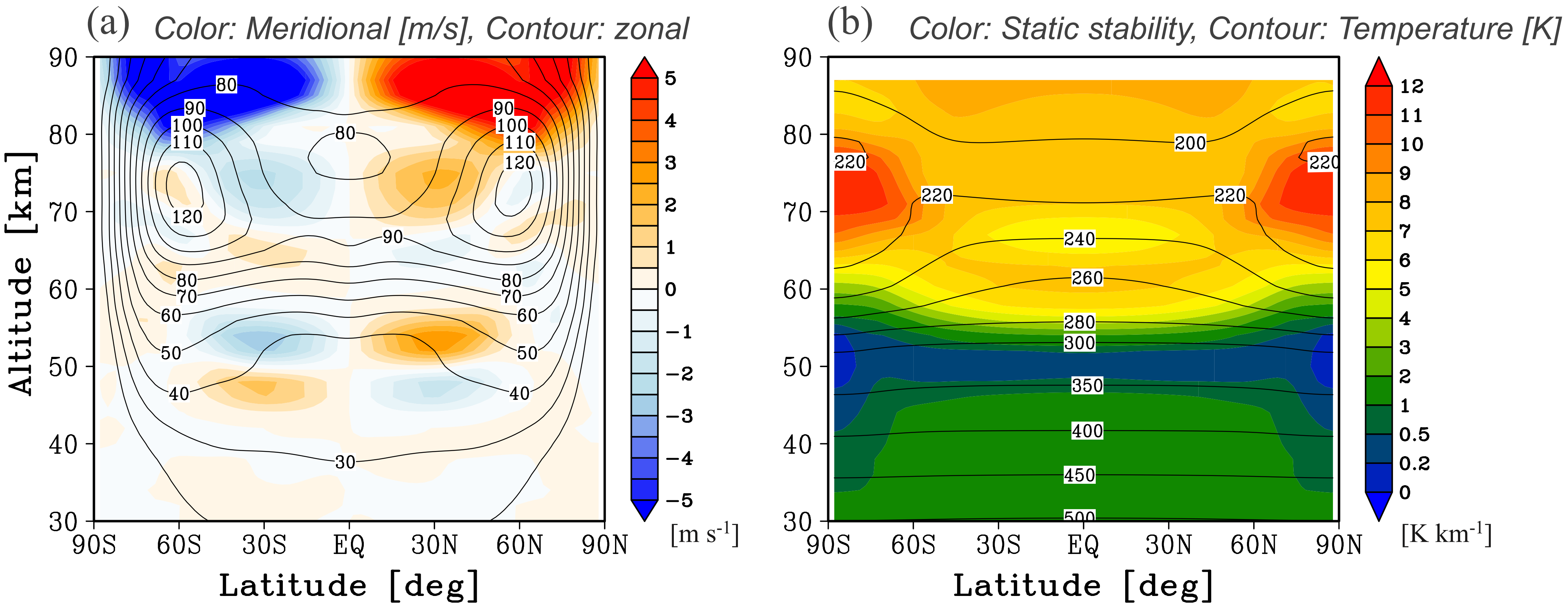

- Atmospheric Superrotation
- Hadley-like circulations

- Consistent with recent observations (Ando et al. 2020)
- Low static stability in the cloud layer

<u>Those structures are similar to Yamamoto et al. (2021)</u>

Zonal mean cloud structure

Color: Mass loading [mg/m^3], Line: Cloud top @1μm

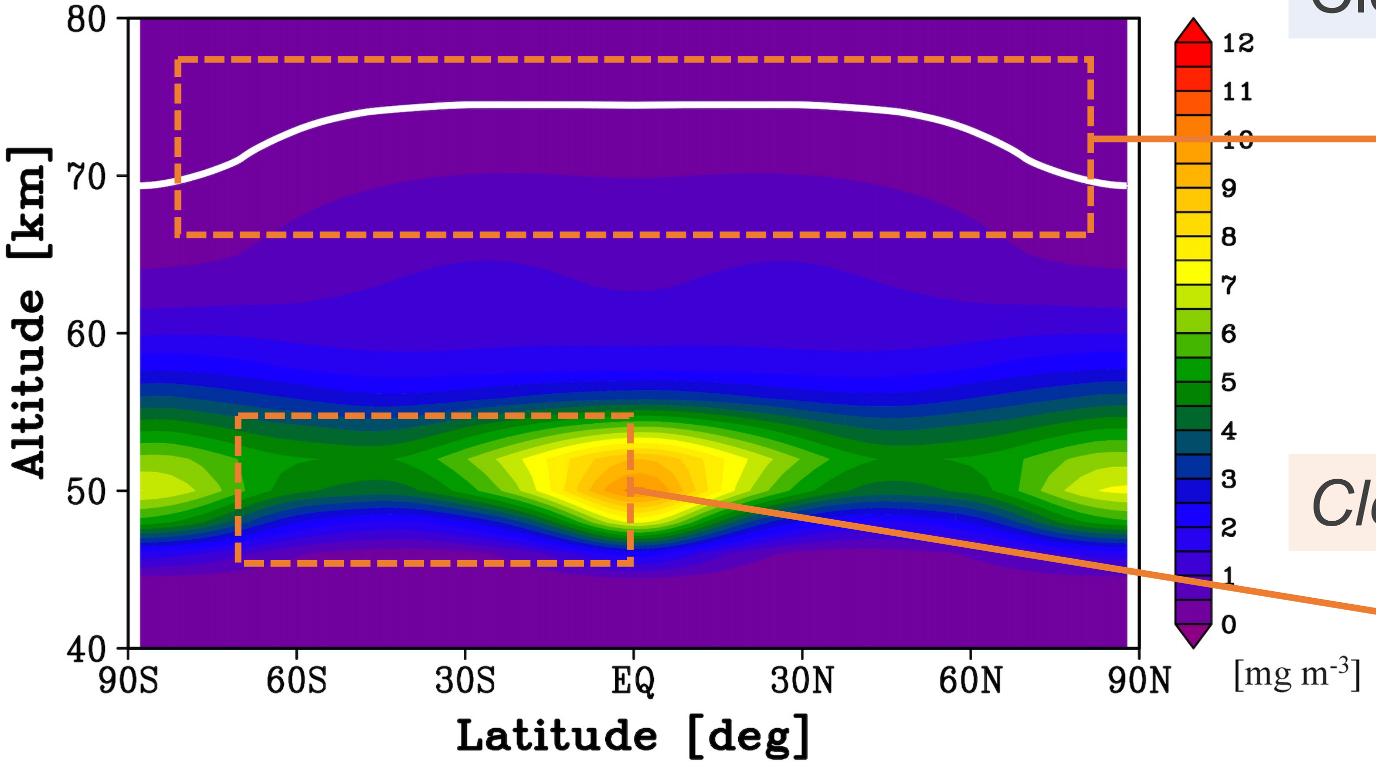

Cloud top

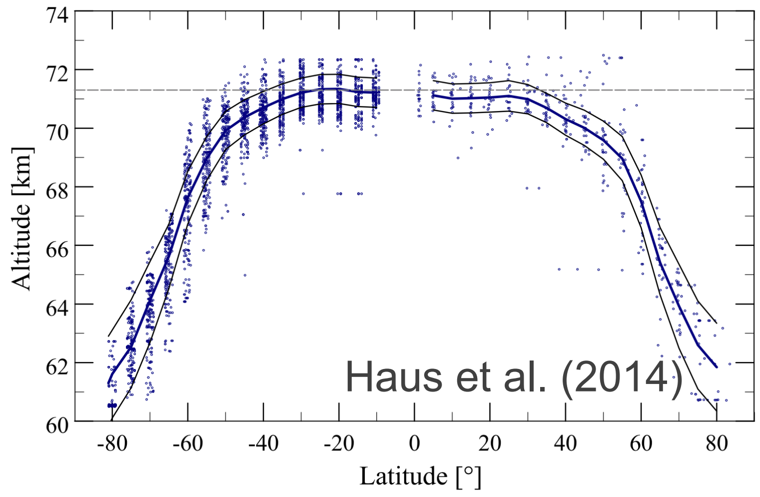

Cloud bottom

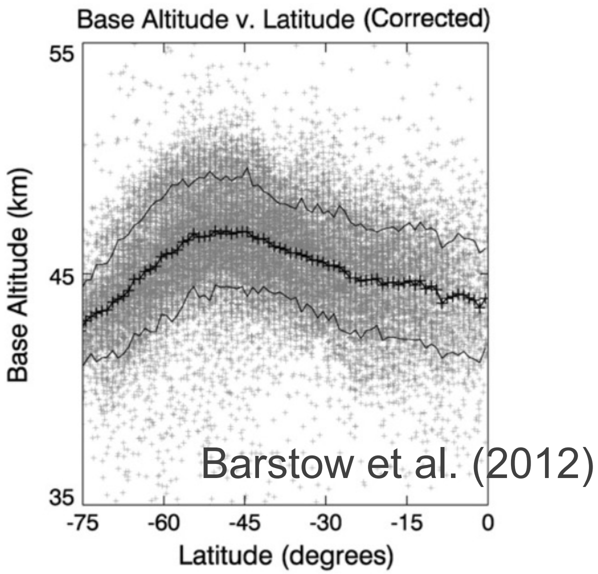

Cloud top and bottom structures are qualitatively consistent with the past near-infrared observations

Cloud variation and an atmospheric wave

Color: Height [m], Contour: COD, Vector: Wind [m/s] @50 km

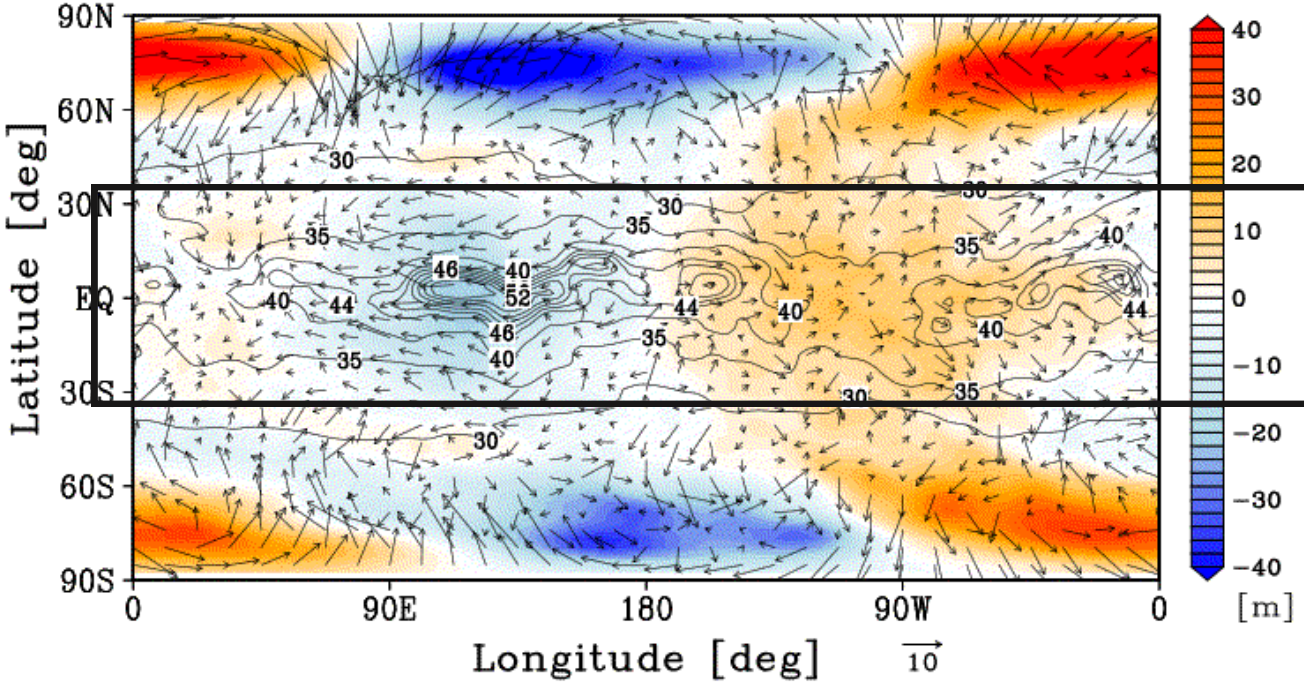

Observation (Crisp et al., 1991)

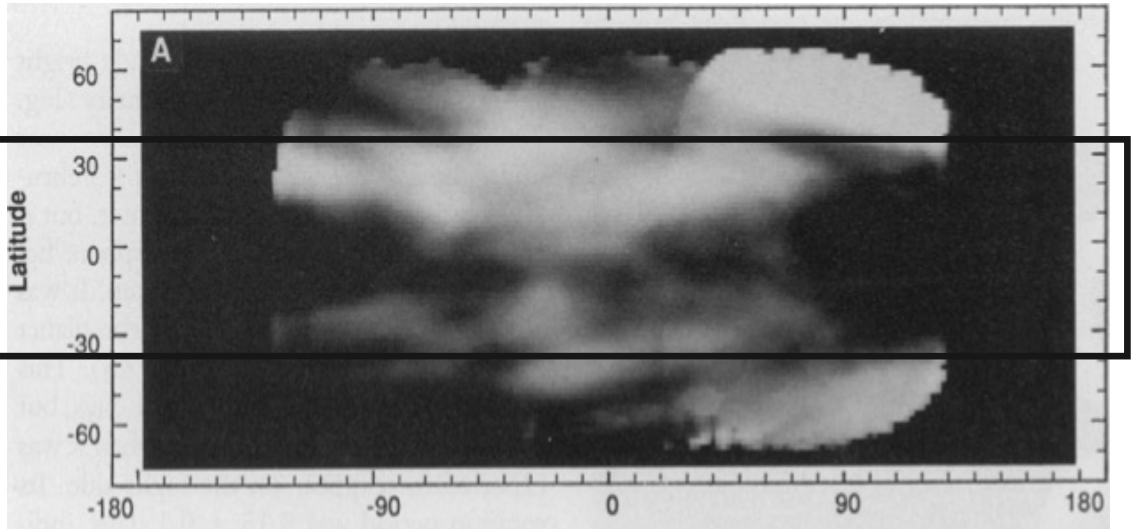

- A zonal-wavenumber-1 Kelvin wave with a planet-circling period of 7.1 days is found in the equatorial region
- Cumulative Optical Depth (COD) variation is caused by the Kelvin wave

→ Similar to the observed opacity variation (Crisp et al., 1991)

Planetary-scale Cloud Variation

We performed composite analysis to highlight the variation related to the Kelvin wave to investigate the variation mechanism

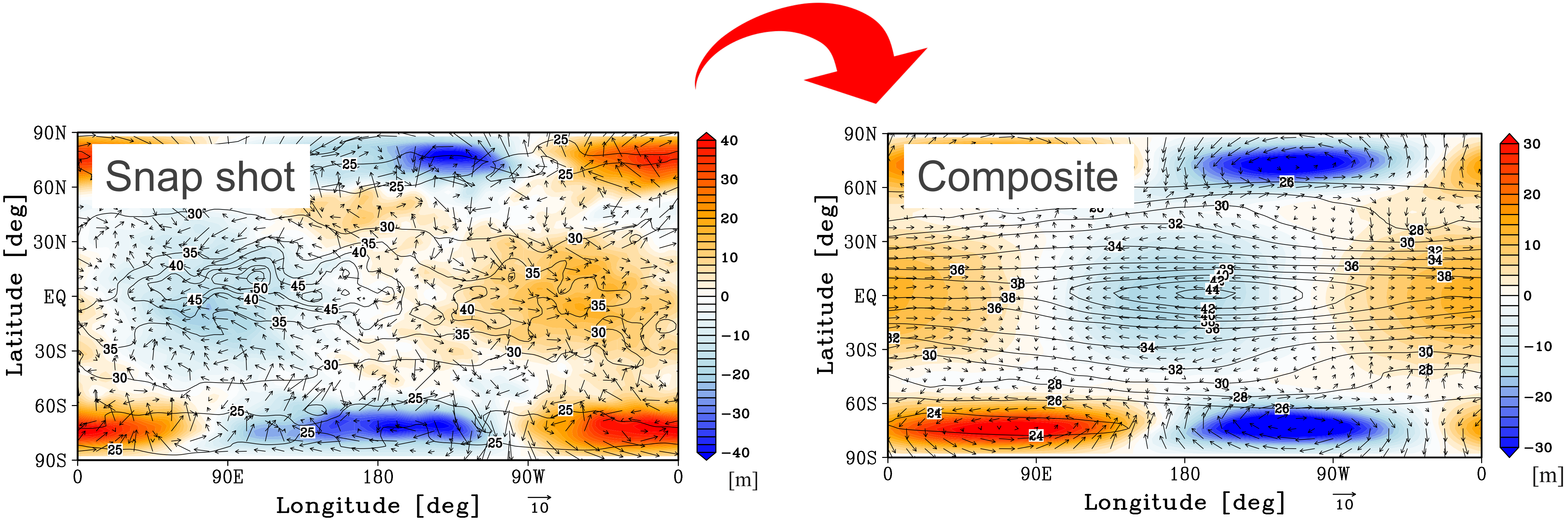

Planetary-scale Cloud Variation

(a) *Color: ML changing rate [mg/m^3/day], Contour: Temperature changing rate [K/day]*

(b) *Color: ML changing rate [mg/m^3/day], Contour: Vertical wind [mm/s]*

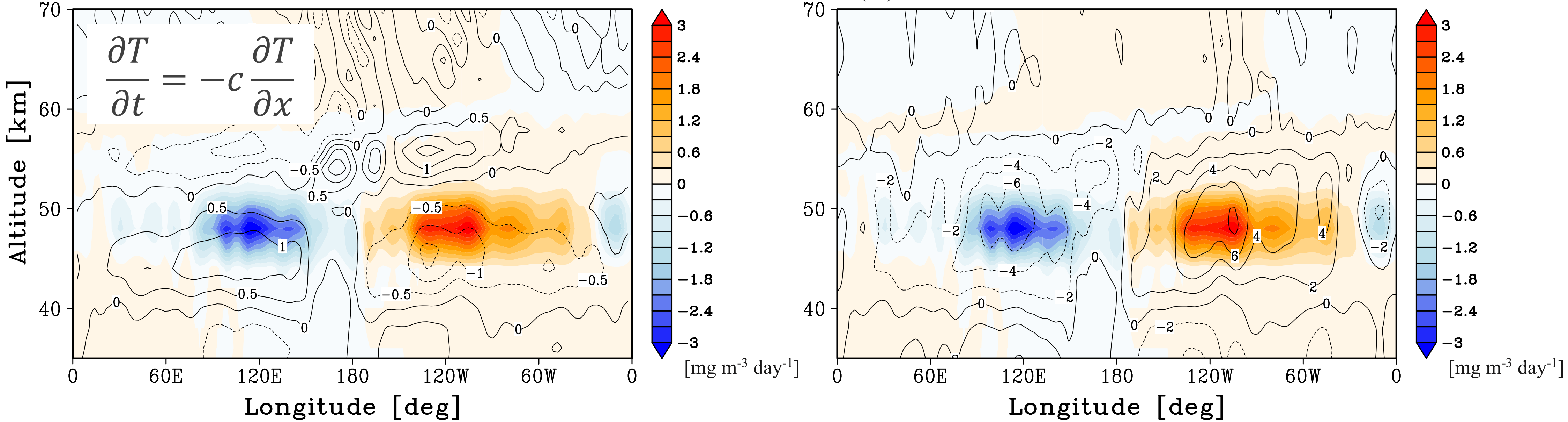

- Mass loading (ML) changing rate by temperature: ~0.8 [mg/day] (calculated with p_{sat} change by $\partial T/\partial t$)
- ML changing rate by vertical wind: ~2.5 [mg/day] (calculated with p_{sat} vertical gradient and vertical wind)

→ Vertical wind is the leading cause of the periodic cloud variation

Comparison with Ando et al. (2021)

Effect of static stability S

Criteria of instability

$$\frac{\partial\theta}{\partial z} = \frac{\partial(\theta_0 + \theta')}{\partial z} < 0$$

S: Stability — Wave amp.

θ: Potential temperature

S controlls the amplitude of temperature variation

Color: Static stability [K/km]

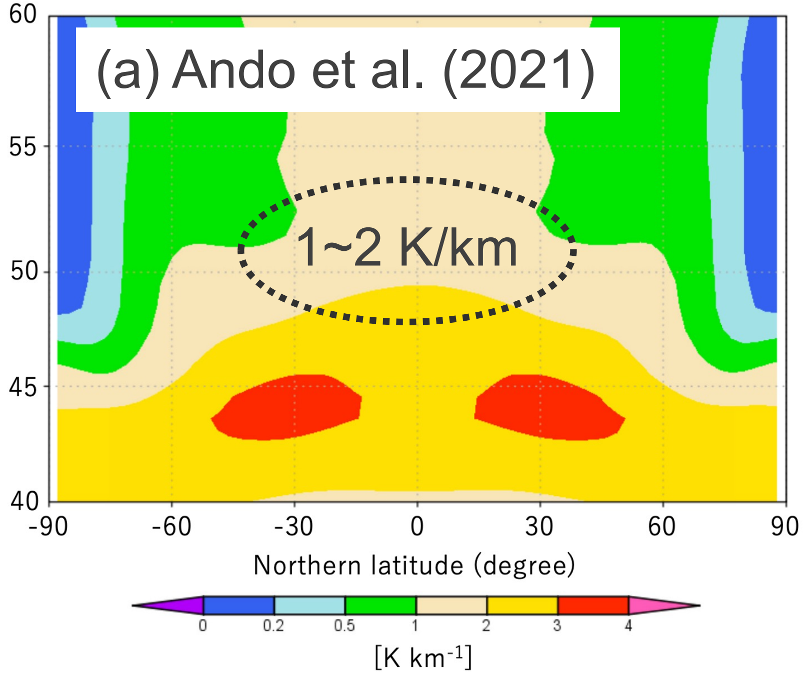

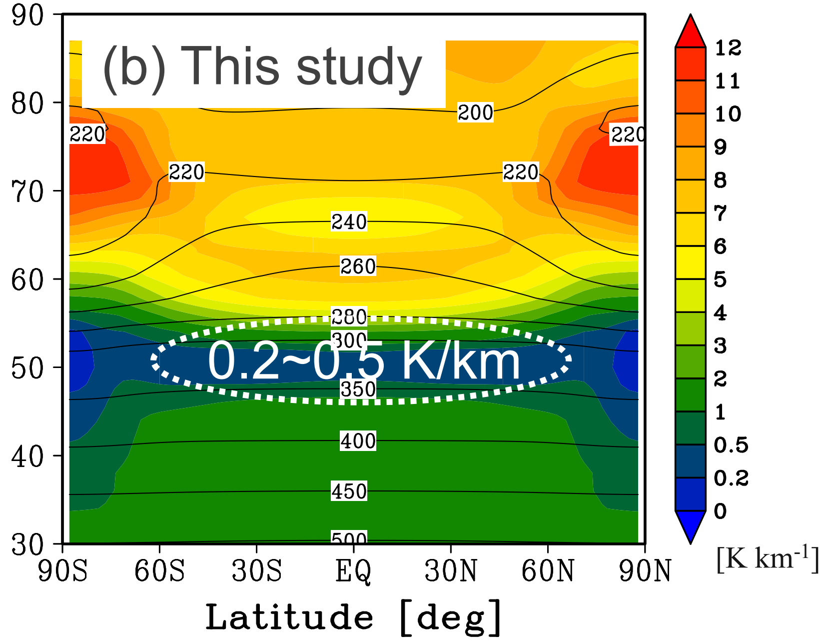

- The simulated stability is lower than Ando et al. (2021)
  → smaller temperature amplitude and larger vertical wind amplitude
  → Cloud variation is controlled by vertical wind
- The difference may be attributed to temperature calculation methods

→ Newtonian cooling (Ando et al.) or Radiative transfer (This study)

Implication for Cloud Morphology

Zonal-wavenumber-1 cloud marking

- Rotation period (7.1 day) is larger than the observation (4.9 ± 0.5 day) because our model underestimates zonal wind speed in the cloud layer

→ Providing the zonal wind speed is the same as the observation, the rotation period agrees with the observation (4.2~5.1 days)

- COD variation associated with the Kelvin wave is 15% of total variation

→ Consistent with 10~25% reported by the past observation (Crisp et al., 1991)

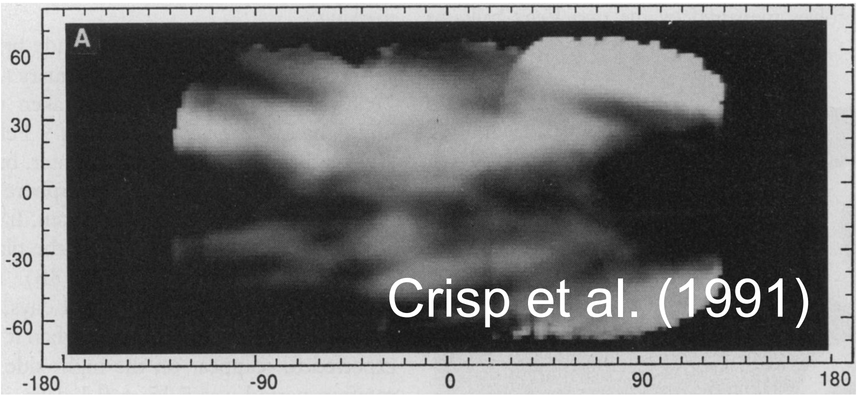

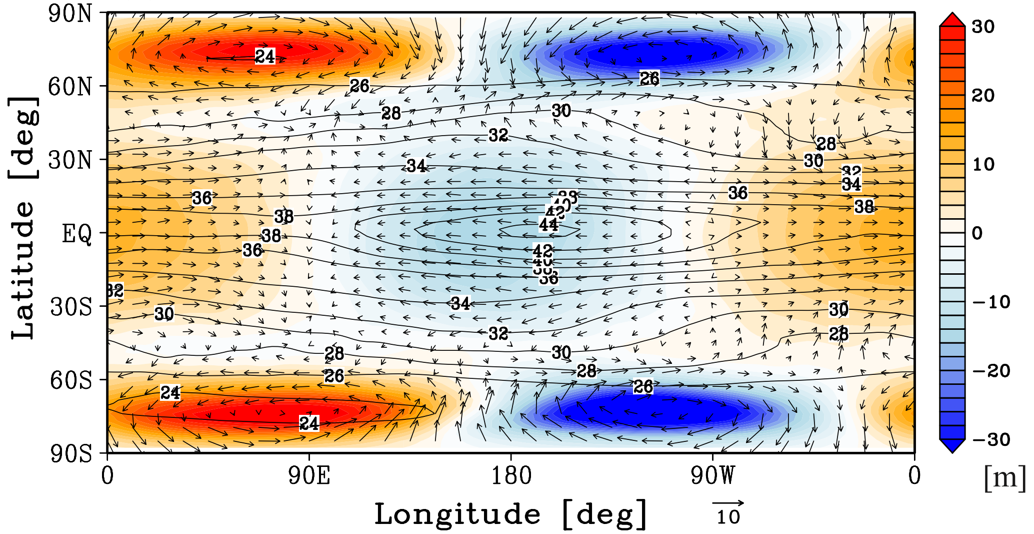

The observed variation can be explained by a Kelvin wave

Conclusions

- We reproduced cloud top and bottom structure consistent with the observation
- We reproduced cloud variation consistent with the observation by including Mode 3 particles
- The cloud variation is coupled with a zonal-wavenumber-1 Kelvin wave
- Kelvin wave vertical wind is essential for maintaining the periodic variation
- Radiative transfer may play an important role on determining the mechanism of cloud variation
- The reproduced cloud variation chrecteristics are in good agreement with the observed wavenumber-1 cloud marking

→ the Kelvin wave can explain the cloud variation in low latitudes

This work has been published (JGR Planets): https://doi.org/10.1029/2022JE007595

References

- Ando, H., Imamura, T., Tellmann, S., Pätzold, M., Häusler, B., Sugimoto, N., et al. (2020b). https://doi.org/10.1038/s41598-020-59278-8
- Ando, H., Takagi, M., Sagawa, H., Sugimoto, N., Sekiguchi, M., & Matsuda, Y. (2021). https:// doi.org/10.1029/2020JE006781
- Barstow, J. K., Tsang, C. C. C., Wilson, C. F., Irwin, P. G. J., Taylor, F. W., McGouldrick, K., et al. (2012). https://doi.org/10.1016/j.icarus.2011.05.018
- Crisp, D., McMuldroch, S., Stephens, S. K., Sinton, W. M., Ragent, B., Hodapp, K. W., et al. (1991). https://doi.org/10.1126/science.253.5027.1538
- Grinspoon, D. H., Pollack, J. B., Sitton, B. R., Carlson, R. W., Kamp, L. W., Baines, K. H., et al. (1993). https://doi.org/10.1016/0032-0633(93)90034-Y
- Haus, R., Kappel, D., & Arnold, G. (2014). https://doi.org/10.1016/j.icarus.2014.01.020
- Hide R. (1969). https://doi.org/10.1175/1520-0469(1969)026<0841:DOTAOT>2.0.CO;2
- Horinouchi, T., Hayashi, Y.-Y., Watanabe, S., Yamada, M., Yamazaki, A., Kouyama, T., et al. (2020). https://doi.org/10.1126/science.aaz4439
- Ikeda, K. (2011). (PhD thesis). The University of Tokyo.
- Kasten, F. (1968). https://doi.org/10.1175/1520-0450(1968)007<0944:FSOAP>2.0.CO;2
- Knollenberg, R. G., & Hunten, D. M. (1980). https://doi.org/10.1029/JA085iA13p08039
- Krasnopolsky, V. A. (2012). https://doi.org/10.1016/j. icarus.2011.11.012
- Krasnopolsky, V. A. (2013). https://doi.org/10.1016/j.icarus.2013.04.026
- Machado, P., Widemann, T., Peralta, J., Gilli, G., Espadinha, D., Silva, J. E., et al. (2021). https://doi.org/10.3390/atmos12040506
- Marcq, E., & Lebonnois, S. (2013). https://doi.org/10.1002/jgre.20146
- Numaguti, A., Takahashi M., Nakajima T., & Sumi A. (1995). Matsuno, Ed., Center for Climate System Research, 1–27.
- Peralta, J., Navarro, T., Vun, C. W., Sánchez-Lavega, A., McGouldrick, K., Horinouchi, T., et al. (2020). https://doi.org/10.1029/2020GL087221
- Takagi, M., Ando, H., Sugimoto, N., & Matsuda, Y. (2022). https://doi.org/10.1029/2021JE007164
- Titov, D. V., Ignatiev, N. I., McGouldrick, K., Wilquet, V., & Wilson, C. F. (2018). https://doi.org/10.1007/s11214-018-0552-z
- Yamamoto, M., Ikeda, K., Takahashi, M., & Horinouchi, T. (2019). Solar-locked and geographical atmospheric structures inferred from a Venus general circulation model with radiative transfer. Icarus, 321, 232-250. https://doi.org/10.1016/j.icarus.2018.11.015
- Yamamoto, M., Ikeda, K., & Takahashi, M. (2021). Atmospheric response to high-resolution topographical and radiative forcings in a general circulation model of Venus: Time-mean structures of waves and variances. Icarus, 355, 114154. https://doi.org/10.1016/j.icarus.2020.114154